

## THERMAL ACCOMMODATION COEFFICIENTS BY HIGH SPEED VIBRATION OF SOLID SAMPLES

### I. Method and apparatus

Richard S. LEMONS and Gerd M. ROSENBLATT

*Department of Chemistry,  
The Pennsylvania State University,  
University Park, Pennsylvania 16802 U.S.A.*

Received 16 August 1974; revised manuscript received 31 October 1974

A method and apparatus to determine thermal accommodation coefficients are described in which solid samples are vibrated at high velocity in the presence of a test gas at low pressure. Energy transfer between the incident gas molecules and the moving surface causes an increase in the solid temperature which is related to, and approximately proportional directly to the thermal accommodation coefficient and inversely to the emissivity. The apparatus may be used over a wide range of temperatures and pressures in the long mean-free-path region with many types and forms of solid samples. Measurements as a function of pressure may yield information on internal energy accommodation, as well as translational accommodation, in favorable circumstances. Results at room temperature for  $O_2$ ,  $N_2$ , and Ar on uncoated and greased Pt, Ni, and Cu surfaces, and on carbon coated Pt are presented.

### 1. Introduction

Thermal accommodation coefficients are of interest in areas such as aerospace materials technology, high altitude flight (drag coefficients) [1], the efficiency of energy conversion devices, heat transfer computations, and gas-solid reaction kinetics. Knudsen [2] introduced the thermal accommodation coefficient  $\gamma$  as a measure of the average degree of thermal equilibration of gas atoms or molecules incident upon, and subsequently emitted from, solid surfaces. In terms of energies  $\gamma$  is defined by

$$\gamma = (E_I - E_R)/(E_I - E_S), \quad (1)$$

where the subscript I refers to incident molecules, R to reflected or reevaporated molecules, and S to molecules thermally equilibrated with the solid surface. Complete thermal equilibration of incident gas molecules with the solid surface,  $E_R = E_S$ ,

yields  $\gamma = 1$  whereas no energy transfer between incident gas molecules and the solid sample  $E_R = E_i$ , yields  $\gamma = 0$ .

Common means of measuring accommodation coefficients are Knudsen low pressure and temperature jump methods [1,3] in which  $\gamma$  is determined from the measured power loss to the gas from a hot filament axially mounted in a cylindrical vessel and maintained at a constant temperature by passing a small electric current through it. In the low pressure method the mean free path of the gas is long relative to the filament and cell dimensions and the entire body of gas may be considered to be at the temperature of the vessel walls. At the higher pressures used in the temperature jump method, typically 10 to 100 Torr, thermal conduction from the filament to the vessel walls introduces temperature gradients in the gas. The total temperature drop between the filament and wall is considered to be divided into a temperature drop from filament to ambient gas (the temperature jump) and a drop through the gas. The theory by which accommodation coefficients are derived from temperature-jump measurements is somewhat precarious [1,3,4]. A calorimetric method to obtain  $\gamma$  was used by Klett and Irey [5] in which the rate of heat transfer by a gas between two solid surfaces at different but constant temperatures is determined from the evaporation rate of liquid nitrogen surrounding the lower temperature surface. Devienne [6] devised a method to measure the ratio of the translational accommodation coefficient to the thermal emissivity  $\epsilon$  by mounting solid samples on the ends of a 1.25 meter arm which is rotated at high velocities.

The present paper reports a new method for measuring thermal accommodation coefficients, development of which was motivated by the rotating arm method of Devienne [6]. In the present method values of  $\gamma/\epsilon$  are determined from the increase in temperature of a solid sample when it is vibrated at high velocity in a stagnant test gas. The sample is mounted on the end of a velocity transformer attached to an ultrasonic transducer and is surrounded by a small furnace which fixes the initial temperature of the sample and of the test gas. Typical temperature increases observed with the apparatus described in this paper are on the order of 0.1 to 2°. Measurements can be made over a wide range of pressures in the low pressure region where the mean free path in the gas is greater than, or on the order of, the interior dimensions of the furnace. The upper restriction to the experimental temperature is determined only by the thermal properties of the adhesive bonding the sample to the velocity transformer, the vapor pressure of the sample, and the ability to measure small temperature differences. These conditions become more restrictive at high temperatures both experimentally and theoretically, since, for a given value of  $\gamma/\epsilon$ , the magnitude of the temperature increase of the vibrating sample decreases with increasing gas temperature at constant pressure. Solid samples may be polycrystalline, single crystal, amorphous, or waxy in state. They may be in the form of foils, wafers, or thin films. Adhesion of the sample to the velocity transformer is the only major experimental difficulty. To ensure that the adhesive bond does not break under the very large accelerations, samples should be no thicker than 0.1 mm. The variety of solid samples which can be used is a major advantage of the method. The choice of mater-

ials for which  $\gamma/\epsilon$  can be measured is not limited, as in the Knudsen low pressure and temperature jump methods, to electrically conducting substances for which filaments are available. An additional advantage of the method is that the measurement is rapid: the maximum temperature rise of the sample is achieved within seconds after power is applied to the ultrasonic transducer. This also means that long-term temperature stability of the furnace is not essential.

Average translational accommodation coefficients for a given gas-surface system at a chosen incident energy and solid temperature may, in principle, be derived from molecular beam studies in which scattered beam spatial and velocity distributions are observed as a function of incident angle [7]. It is sometimes difficult to ensure that all reemitted molecules are observed with equal probability in beam experiments. For this and other reasons it is not always easy to "normalize" molecular beam results to the average behavior of incident gas. Thus, it is helpful to compare molecular beam results with  $\gamma$  values representative of molecules incident over all angles and a Maxwellian distribution of molecular velocities. The vibrating solid method, which uses the same kinds of samples as molecular beam studies, may be a useful way to obtain such comparative data.

Since the ratio  $\gamma/\epsilon$  is measured by the method reported in this paper the thermal emissivity of the sample must be known in order to obtain  $\gamma$ . On the other hand, values of  $\gamma/\epsilon$  are useful directly in some engineering applications [8,9]. In most other methods to determine thermal accommodation coefficients  $\gamma$  depends upon an additional parameter, such as the thermal conductivity of the gas.

## 2. Principle of method

The solid sample is vibrated at ultrasonic frequency, with a maximum velocity approaching thermal molecular velocities, in the presence of a stagnant test gas at low pressure. The test gas density should be low enough that the mean free path in the gas is greater than about three times the distance between the sample surface and the furnace wall. This corresponds approximately to pressures less than  $10^{-3}$  torr. Under these conditions, usually described as the "molecular flow regime" [8,10], the number of gas phase collisions is negligible compared to the number of gas-surface collisions and the average molecular velocity in the gas is determined by the temperature of the furnace walls  $T_G$ .

The sample vibrates normal to its exposed face. Before vibration begins the surface is stationary in the lab-frame, and those molecules colliding with the sample impart a kinetic energy flux of  $2kT_G$  times the incident molecular flux. Once vibration begins, as the sample moves in through the gas, the incident molecular velocity relative to the sample is greater than the lab-frame velocity. In that case the translational temperature of the gas is enhanced from the viewpoint of the solid, which results in relative kinetic energy being transferred from incident gas molecules to the solid. Alternatively, as the solid recedes through the gas the situation is reversed. Those

molecules that collide have incident velocities relative to the solid less than the lab-frame velocity, resulting in transfer of relative kinetic energy from solid to gas. However, more collisions occur while the solid is moving in through the gas than while it is receding. With the solid velocities achieved in the present apparatus ( $\sim 3 \times 10^4$  mm sec $^{-1}$ ), this excess is approximately 35%. The net result is transfer of relative energy from gas to vibrating surface which causes the sample temperature to increase.

The sample temperature stabilizes at a value below that which characterizes the incident molecules from the viewpoint of the solid because of thermal radiation from the solid to the walls of the vessel. That is, thermal emission causes the thermal energy characteristic of the surface,  $E_S$  in eq. (1), to remain below the apparent thermal energy of incident gas molecules  $E_I$  even after steady-state is attained. Conservation of energy requires that

$$\Delta E = 0 = E_I - E_R - E_E \quad (2)$$

The symbol  $E_E$  represents the thermal emission energy from unit area per second:

$$E_E = \sigma \epsilon (T_S^4 - T_G^4) \quad (3)$$

where  $\sigma$  is the Stefan-Boltzmann constant. Heat conduction is slow along the titanium alloy rod on which the sample is mounted and may be neglected. The thermal energy characteristic of the surface,  $E_S$  in eq. (1), is the total relative kinetic energy flux leaving unit area of surface if every gas molecule which strikes the surface equilibrates thermally with the surface. From kinetic theory

$$E_S = 2kT_S J_I \quad (4)$$

where  $J_I$  is the average flux density of molecules incident upon, and reemitted from, the oscillating surface.

Combining eqs. (1) through (4) yields

$$\gamma/\epsilon = \sigma (T_S^4 - T_G^4) / (E_I - 2kT_S J_I) \quad (5)$$

The cause of the rise in temperature of the vibrating sample is the increased relative kinetic energy of incident gas molecules when the oscillating surface moves into the gas. In order to obtain  $\gamma/\epsilon$  from steady-state measurements of the temperature rise,  $\Delta T = T_S - T_G$ , one must calculate the appropriate values of  $J_I$  and  $E_I$  to use in eq. (5). The following paper [11] employs the kinetic theory of gases to develop equations for the flux and relative kinetic energy incident upon an oscillating solid, averaged over times long compared to a vibration cycle.

The kinetic theory development for the high-speed vibration apparatus [11] is not quite the same as that applicable to Devienne's rotating arm apparatus [6]. Two effects cause the incident flux, and the distribution of incident molecular velocities, seen by the oscillating solid to differ from that seen by (both sides of) a wafer continuously moving in one direction: (1) The incident flux *directly from the gas* is deficient in slow moving molecules during the second half of a vibration cycle, in which

the surface moves into the gas, because, when the surface moves away from the gas, it vacates a volume which some molecules are too slow to refill before the surface moves into the gas. Neglecting end effects, molecules from the gas which hit the surface during a given cycle have to cross the plane of maximum sample extension during that same cycle. (2) The oscillating solid, in addition to colliding with molecules directly from the gas, also collides with slow-moving molecules emitted from the surface earlier in the cycle if the surface catches up with these before they escape from the volume swept out by the solid. These two effects act in opposite directions and compensate to a large degree. However, the first effect predominates. In the present experiments "second collisions" represent about 0.7% of the total number of gas-surface collisions. The net result of the two opposing effects is that the temperature increase of an oscillating solid is about 10% greater than that of a continuously moving wafer of the same root-mean-square velocity [11].

The kinetic theory development [11] shows that the incident flux and relative translational energy which describe the vibration apparatus are

$$J_1 = N(4\pi a) - 1/2 + [a_S u^2 - (7/6)(a_S u^2)^2] J_1(u+) \quad (6)$$

and

$$E_1 = N[(4\pi a) - 1/2] \{ \frac{1}{2} m u^2 + 2kT_G \} + \frac{1}{2} m u^2 J_1(u+) \quad (7)$$

The first term in eq. (6) is  $J_1(0)$ , the flux incident upon unit area of stationary surface. The last terms in eqs. (6) and (7) represent, respectively, the incident flux  $J_{11}$  and relative kinetic energy  $E_{11}$  associated with "second collisions". The symbol  $J_1(u+)$  represents the average flux incident upon an oscillating surface during the recession half of a vibration cycle:

$$J_1(u+) = N \{ (4\pi a) - 1/2 \exp(-au^2) - \frac{1}{2} u [1 - \operatorname{erf}(u\sqrt{a})] \} \quad (8)$$

The other symbols which appear in eqs. (6) to (8) are:  $N = P/kT_G$  is the molecular number density;  $a = m/2kT_G$  and  $a_S = m/2kT_S$ ;  $m$  is the molecular mass of the test gas;  $u = u_m/\sqrt{2}$  is the root-mean-square velocity of the vibrating surface; and  $\operatorname{erf}$  represents the error function.

During an experiment the pressure of the known test gas is measured with an ionization gauge, and the temperature of the gas  $T_G$  and temperature increase of the solid sample  $\Delta T = T_S - T_G$  are determined from thermocouple measurements. Ratios of  $\gamma/\epsilon$  can then be calculated from eq. (5) using eqs. (6) through (8). Figs. 1 through 3 illustrate the magnitude of the temperature rise expected for argon under various conditions. As illustrated in fig. 2,  $\Delta T$  varies approximately as  $u^2$ . Figs. 1 and 3 show that, with the solid velocities achieved with the present apparatus, there are a large combination of circumstances which give rise to temperature increases in excess of  $0.1^\circ$ , increases which are large enough to yield useful measurements of  $\gamma/\epsilon$ . In the calculations shown in figs. 1 to 3 the sinusoidal oscillation of the surface has been approximated by a sawtooth oscillation of the same root-mean-square velocity [11]. Calculations neglecting second collisions show that the sawtooth oscillator

yields ratios of  $\gamma/\epsilon$  in agreement to about one part in a thousand with the results computed for a sinusoidal oscillator if  $u < 10^3$  mm sec $^{-1}$  and  $\Delta T < 10^\circ$ .

In the limit approached with samples of very low emissivity,  $\gamma/\epsilon \rightarrow \infty$ ,  $E_S$  becomes equal to  $E_1$ , and  $T_S$  becomes equal to  $E_1/2kJ_1$ . At this limit  $T_S = T_G + \Delta T$  is simply a measure of the apparent average translational temperature of the gas from the reference frame of the moving surface. In this case,  $\Delta T$  is independent of gas pressure in the molecular flow (high Knudsen number) regime (fig. 1). Although  $\Delta T$  is maximized under these conditions,  $\Delta T$  is independent of the efficiency of energy transfer in the gas-surface collisions so that no information regarding  $\gamma$  can be obtained from measurements of the temperature rise. In this limit,  $\Delta T$  is essentially independent of  $T_G$  (it decreases very slightly with  $T_G$ , see fig. 3) and varies essentially as  $mu^2$  (fig. 2). The maximum temperature rise computed for argon at 300 K and  $10^{-3}$  torr, with  $u = 3.3 \times 10^4$  mm sec $^{-1}$  as achieved in the present apparatus, is  $2.9^\circ$ .

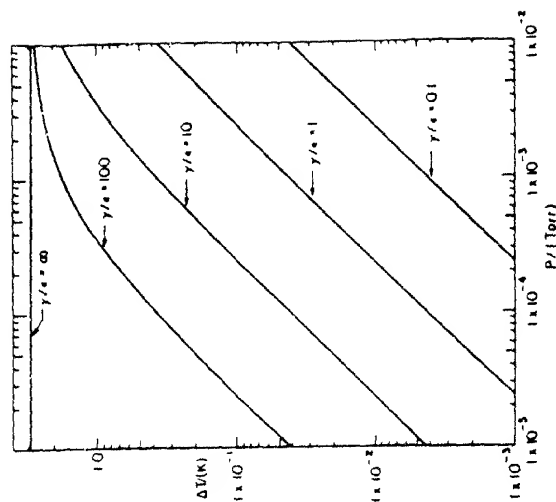


Fig. 1. Calculated effect of test gas pressure (assuming molecular flow) upon the temperature increase of a vibrating solid. The different lines correspond to various ratios of translational thermal accommodation coefficient to emissivity with the same incident gas, assuming negligible internal accommodation. The numerical values refer to argon at 300 K and assume a root-mean-square sample velocity of  $u = 3.3 \times 10^4$  mm sec $^{-1}$ .

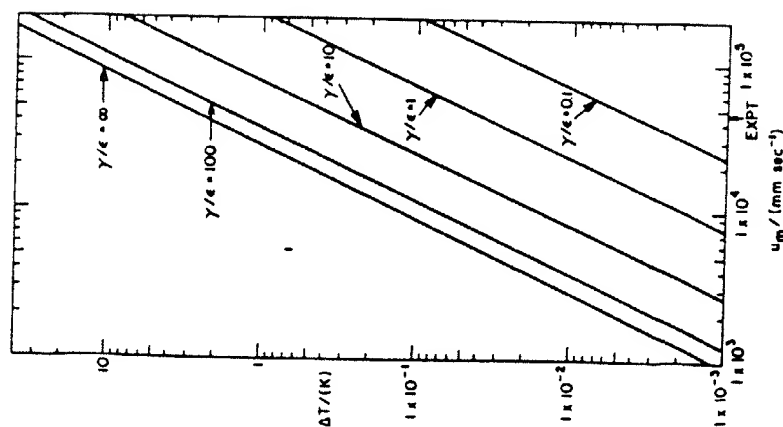


Fig. 2. Calculated effect of sample velocity upon the temperature increase of a vibrating solid. The different lines correspond to various ratios of translational thermal accommodation coefficient to emissivity with the same incident gas, assuming negligible internal accommodation. The numerical values refer to argon at 300 K and  $10^{-3}$  torr. The arrow marked EXPT shows the value of  $u_m$  attained with the present apparatus.

At higher radiative emissivities the temperature increase varies inversely as the emissivity. Under these conditions  $\Delta T$  is approximately directly proportional to the pressure, as illustrated in fig. 1, and to the thermal accommodation coefficient  $\gamma$ . When the temperature increase is small,  $\Delta T$  is approximately proportional to  $T_G^{-5/2}$  (fig. 3), to  $m^{1/2}$ , and to  $u^2$  (fig. 2). The rapid decrease in  $\Delta T$  as the system temperature increases is caused by the  $T^4$  increase in thermal emission from the sample surface.

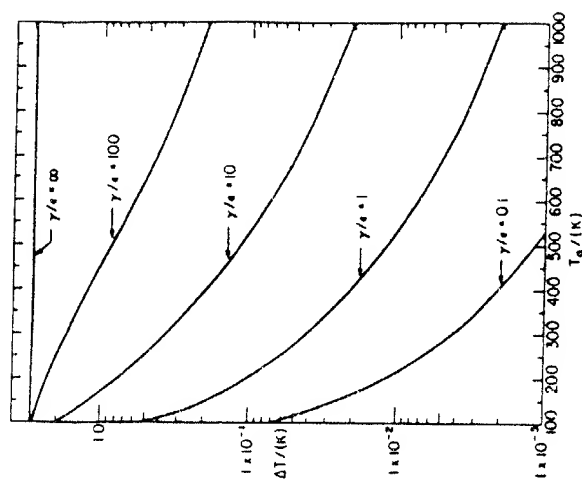


Fig. 3. Calculated temperature increase of a vibrating solid as a function of gas temperature. The different lines correspond to various ratios of translational thermal accommodation coefficient to emissivity with the same incident gas, assuming negligible internal accommodation. The calculations assume  $u = 3.3 \times 10^4$  mm sec $^{-1}$  and are for argon at a constant density ( $3.2 \times 10^{14}$  molecules mm $^{-3}$ ) equal to that at 300 K and  $10^{-3}$  Torr.

In considering the interaction of molecules rather than atoms with solid surfaces, internal energy exchange may be significant. Although rotational-translational energy transfer may occur during collision with a solid [12], vibrational energy changes are much less probable since the vibrational energy level spacings are usually on the order of, or larger than,  $kT$ . The orientation of the incident molecules may also affect the gas-solid interaction. For the diatomic molecular gases used at room temperature in this work only rotational and translational energy changes during gas-solid collisions will be considered.

The rotational kinetic energy incident upon unit area in unit time which can be added to the relative translational energy of incident molecules given by eq. (7), is, for diatomic molecules:

$$E_1(\text{rot}) = J_1 k T_G \quad (9)$$

Similarly, the rotational energy to be added to the translational energy of thermally equilibrated diatomic molecules, eq. (4), is

$$E_S(\text{rot}) = J_1 k T_S \quad (10)$$

If one assumes that  $\gamma(\text{trans}) = \gamma(\text{rot})$  as a limiting case (this approximation appears probable only when there is essentially complete accommodation,  $\gamma \approx 1$ ) eqs. (5), (9), and (10) may be combined to yield

$$\gamma/\epsilon = \alpha(T_S^4 - T_G^4)/[E_1 - J_1 k(3T_S - T_G)] \quad (11)$$

where  $J_1$ , eq. (6), and  $E_1$ , eq. (7), represent the incident flux and the incident relative translational kinetic energy, as before. For a rigid, nonlinear molecule the term  $3T_S - T_G$  in eq. (11) is replaced by  $(7T_S/2) - (3T_G/2)$ .

Since the incident internal energy is unaffected by the sample motion, any internal energy transfer is from the solid to the gas, and thus tends to reduce the extent to which the solid temperature increases upon vibration. In favorable circumstances to which the difference between eq. (5) and (11) may be used to extract information on the difference between  $\gamma(\text{trans})$  or  $\gamma(\text{rot}) \approx 0$  by measuring  $\Delta T$  for a given gas and surface at different gas pressures. Calculation of a constant value of  $\gamma/\epsilon$  from eq. (11) from measurements at different pressures indicates that  $\gamma(\text{trans}) \approx \gamma(\text{rot})$ . Calculation of a constant value of  $\gamma/\epsilon$  from eq. (11), indicates that  $\gamma(\text{rot}) \ll \gamma(\text{trans})$  and that the computed value is a measure of  $\gamma(\text{trans})$ . Some of the results presented below for  $O_2$  and  $N_2$  illustrate the latter possibility. Further analysis indicates that, in the intermediate case, under favorable circumstances, measurements of  $\Delta T$  as a function of gas pressure may be analyzed to obtain values for both  $\gamma(\text{trans})$  and  $\gamma(\text{internal})$  [13]. This possibility arises because, while the degree of translational energy exchange is proportional to the incident flux, the degree of internal energy exchange depends upon both the incident flux and the temperature increase of the solid due to translational energy transfer. The internal energy exchange, therefore, increases with the square of the incident flux [13].

### 3. Description of apparatus

The vibrating system, shown in fig. 4, consists of a high efficiency, automatic tuning, magnetostriction, ultrasonic transducer, mounted in a light alloy, water cooled jacket, and a generator (Type WT10/USG10/C, Radyne Limited, Wokingham, Berkshire, England) [14]. The transducer operating at 19.1 kHz resonance frequency with maximum output power of 1 kW produces a 0.038 mm peak-to-peak displacement over the 507 mm<sup>2</sup> face of the stepped coupling stub embodied in the transducer unit and forming the first stage of mechanical amplification. A velocity transducer connected to the output face of the stepped stub amplifies the vibrational displacement by a factor of about twenty. The velocity transducer is a fourth-order, Fourier series, amplitude transformer, similar in overall shape to a long neck

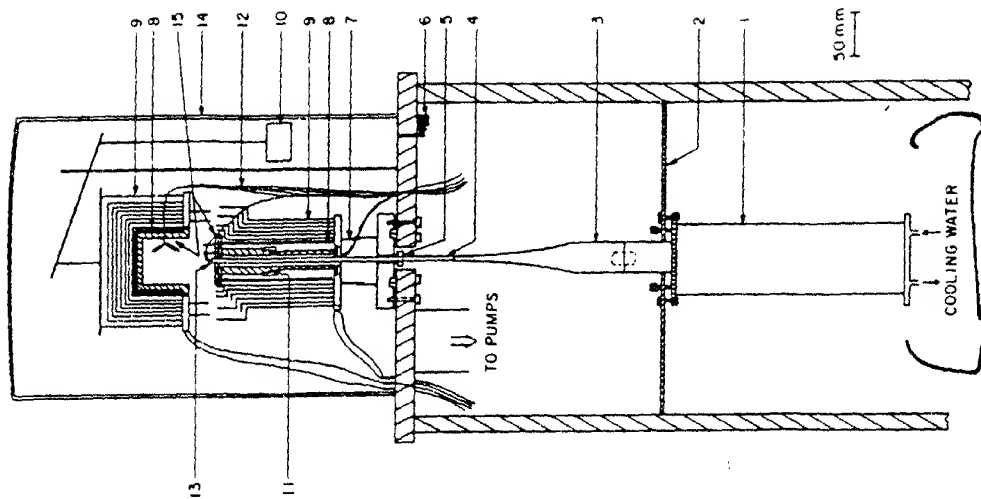


Fig. 4. High speed vibration apparatus. (1) ultrasonic magnetostrictive transducer, (2) mounting bracket, (3) fourth-order, Fourier series amplitude transformer (horn), (4) one wavelength extension rod, (5) vacuum feedthrough, (6) gas leak valve, (7) adjustable aluminum sleeve, (8) ceramic enclosed furnace windings, (9) titanium radiation shields, (10) magnetic counter weight, (11) incoherent diaphragm at nodal plane, (12) chromel-alumel thermocouples, (13) sample, (14) glass bell jar, (15) aluminum furnace.

wine bottle, 180.7 mm in length (0.70 wavelengths) with circular input (34.8 mm diam.) and output (5.0 mm diam.) faces. The transformer (horn) is constructed from IMI titanium 318A alloy (6% Al–4% V) using the theory and design method of Eisner [15].

In order to vibrate the sample inside a furnace in a vacuum system, a one wavelength titanium alloy extension rod 256.5 mm long and 5.0 mm diam. was welded by the ac argon-arc process to the output end of the velocity transformer, thus transferring its vibrational output one wavelength to the free end of the extension rod. The solid sample is attached to the end of the extension rod with an adhesive. The commercial products, Eccobond 104, Eastman 910 and 910 MHT, and Zip-Grip adhesives have been effective in this application at temperatures near room temperature. With 1 kW generator output at 19.1 kHz the peak-to-peak sample displacement amplitude is 0.81 mm, the rms velocity is  $3.3 \times 10^4 \text{ mm sec}^{-1}$ , and the accelerations reach  $6 \times 10^5 \text{ g}$ .

Two nodal planes exist in the extension rod, one-quarter wavelength from each end, at which no motion occurs. These planes are suitable positions for making contact with other materials, although rod alignment is critical. At the nodal plane nearest the velocity transformer the extension rod protrudes through a viton-O-ring vacuum seal in the baseplate of the bell jar vacuum chamber and into the lower section of the vacuum furnace where an Inconel diaphragm forms a seal at the second nodal plane of the extension rod.

The two section aluminum furnace can be pumped out and degassed before magnetically lowering the counterbalanced upper cylindrical section, 5 cm i.d., onto the polished lower surface. The lower furnace section consists of two pieces which clamp the diaphragm on the extension rod between a copper O-ring and an aluminum washer. There are three separate heating elements, each consisting of helically wound resistance coils in an alumina support: one cylindrical element covers the top furnace section, another surrounds the top of the extension rod, while a flat circular element heats the base of the sample region. Each furnace section is surrounded by six titanium foil radiation shields. The furnace temperature is constant to less than  $\pm 0.02^\circ$  for ten minutes and  $\pm 0.1^\circ$  for 1 hr. The maximum furnace temperature is 933 K, the melting point of aluminum.

Sample temperature changes are determined from differences in emf of a 0.051 mm diameter chromel–alumel K thermocouple resting on the solid and an identical thermocouple in contact with a stationary solid near the sample. Other chromel–alumel K thermocouples are positioned throughout the furnace. Differential thermocouple emfs are measured to 30 nV resolution (approximately  $0.0001^\circ$ ), with a Keithley model 180 Digital Nanovoltmeter or model 140 Precision Nanovoltmeter DC Amplifier with a model 662 Guarded DC Differential Voltmeter and absolute temperatures are measured to four digits. Thermocouples were calibrated at the melting point of tin and boiling point of water.

The 50 liter glass bell jar vacuum system is pumped on by a  $690 \text{ l sec}^{-1}$  oil diffusion pump with a water cooled cold trap and is capable of achieving pressures in the  $10^{-7}$  torr range but normally operates in the low  $10^{-6}$  torr range as measured with

a Bayard–Alpert type ionization gauge. A leak valve is used to adjust the test gas pressure which is normally at least two orders of magnitude above background.

The sample velocity  $v_m$  is calculated from the displacement amplitude and oscillation frequency at the output stub of the horn or extension rod prior to installation in the vacuum system [14]. Amplitudes and frequencies are measured using conventional broadcast audio-distortion and harmonic-measuring frequency-modulation apparatus. The transducer is a variable reluctance vibration pickup coil mounted on a dial type micrometer stand [16].

#### 4. Procedure

Samples preferably should be flat and circular with a diameter similar to that of the extension rod. Sample thickness is limited by the mass which the adhesive bond will hold when subjected to large accelerations during vibration. Generally the samples should not be thicker than 0.10 mm.

In preparation for a measurement samples are thoroughly cleaned, care being taken to remove oxide films which would prevent the formation of a strong adhesive bond, bonded to the extension rod, baked to set the adhesive, and re-cleaned. The velocity transformer and sample are then installed in the vacuum system. The height is adjusted, thermocouples are positioned, and the system is evacuated. The furnace may be heated to aid in degassing of the sample. After a pressure below  $10^{-6}$  torr is achieved the system is purged with test gas for several minutes before closing the furnace. Sample and reference temperatures are monitored to ensure that the temperatures are stable and the system is in thermal equilibrium. Sample and reference thermocouples are then bucked against one another so that the temperature change of the sample during vibration is measured.

After a constant test gas pressure is attained, the transducer is powered for two to ten seconds, tuning the transducer if necessary. The temperature change of the solid is monitored on a recorder. Normally the transducer power is repeatedly cycled on and off for two to four second intervals so that a number of measurements are made in rapid succession. The transducer is also powered with no test gas present as a check and calibration.

If the transducer is powered continuously beyond about 30 sec the adhesive bond holding the sample to the extension rod may weaken from the large oscillatory accelerations, thus causing the sample to fly off. Poor bonds can result from improper curing or insufficient aging of the adhesive, as well as from failure to thoroughly clean and remove oxide and grease films from the extension rod and sample surfaces prior to bonding.

The rise in temperature of the sample begins within  $\frac{1}{4}$  sec after applying power to the transducer and reaches a steady-state value in 2–5 sec. With the digital voltmeter, emf measurements can be made as often as every  $\frac{1}{4}$  sec. After the transducer is turned off the surface temperature drops in a few seconds to a temperature usually slightly

greater than the surface temperature before the measurement. This small temperature increase in the solid before and after the measurement comes from power losses in the velocity transformer and occurs at rates much slower than the rapid temperature increase of the sample due to gas-surface energy transfer.

The measurements reported in table 1 were performed on high purity polycrystalline copper 0.0076 mm thick, 0.013 mm platinum, and 0.081 mm nickel foils [14]. Samples were initially cleaned using dilute nitric or hydrochloric acid, followed by successive treatments in an ultrasonic bath with trichloroethylene, MICRO, distilled water, and GC-spectrophotometric quality methanol. For Ni and Cu, Zip-Grip or Eastman 910 adhesive was used, while for Pt, Eccobond 104 was used to bond the samples to the velocity transformer. After the initial adhesive set time of about 2 min, the metal horn and sample were placed in an oven at 315 K for 24 hr. Samples were cleaned as previously upon removal from the oven. In addition, the platinum samples, but not those of copper or nickel, were baked out in the vacuum system for 6 hr at 450 K prior to measurements. Room temperature measurements for Cu and Ni were performed without the use of the extension rod. In addition to measurements on uncoated surfaces, Apiezon M high vacuum grease was applied to each sample to increase the accommodation coefficient towards unity. The platinum sample was also coated with carbon to increase the emissivity to unity. Ion gauge sensitivity for  $O_2$  and Ar relative to  $N_2$  was taken from the literature [17,18].

Table 1  
Representative temperature increases measured at different gas pressures

Surface	$\Delta T$ (K) <sup>a</sup>					$P$ ( $10^{-3}$ torr)				
	$N_2$	$O_2$	Ar	$N_2$	$O_2$	$N_2$	$O_2$	Ar	$N_2$	$O_2$
Platinum uncoated	0.322	0.387	0.302	0.82	0.80	0.82	0.80	0.40		
grease coated	0.379	0.463	0.971	1.0	1.0	1.0	1.0	1.8		
	0.062	0.128	0.153	0.42	0.80	0.42	0.80	0.80		
carbon coated	0.169	0.268	0.351	1.2	1.8	1.2	1.8	2.0		
Nickel uncoated	0.052	0.044	0.056	1.6	1.2	1.6	1.2	1.4		
grease coated	0.064	0.063	0.080	2.0	1.6	2.0	1.6	2.0		
	0.285	0.184	0.371	0.80	0.42	0.80	0.42	0.62		
Copper uncoated	0.398	0.663	0.791	1.2	2.0	1.2	2.0	1.6		
grease coated	0.216	0.227	0.265	0.66	0.64	0.66	0.64	0.60		
	0.492	0.440	0.665	1.8	1.4	1.8	1.4	1.8		
Copper uncoated	0.297	0.427	0.245	0.44	0.48	0.44	0.48	0.20		
grease coated	0.633	1.091	1.340	1.2	2.0	1.2	2.0	2.0		
	0.102	0.163	0.145	0.80	1.2	0.80	1.2	0.90		
	0.193	0.258	0.302	1.6	2.0	1.6	2.0	2.0		

<sup>a</sup>  $\Delta T = T_S - T_G$ ;  $T_G$  varied from 294.6 to 298.0 K, see ref. 14.

## 5. Results and discussion

Table 1 contains examples of results with copper, platinum, and nickel foils using prepurified grade argon, nitrogen, and oxygen gases at room temperature at pressures between  $2 \times 10^{-4}$  and  $2 \times 10^{-3}$  torr [14]. Temperature increases of the uncoated metals, which were clean in the engineering sense but not the surface science sense, range from 0.2 to 1.3°. Coating the surfaces with a very thin layer of vacuum grease to raise the accommodation coefficient towards unity caused the temperature rise to drop to the range 0.06 to 0.7°, because the radiative emissivity was also increased. The carbon-coated platinum surface, presumed to have an emissivity of unity, showed the smallest temperature increase, 0.04 to 0.08°.

The  $\gamma/\epsilon$  ratios and thermal accommodation coefficients calculated from the measurements in table 1 using eq. (5) are shown in table 2. The emissivities of the uncoated surfaces are estimated from literature values [19,20]. The emissivities of the greased samples are estimated from the measured values of  $\gamma/\epsilon$  for Ar assuming  $\gamma = 1$ .

Within the experimental reproducibility of better than 5%, values of  $\gamma/\epsilon$  computed from eq. (5) (see table 2) are independent of the pressure of Ar,  $N_2$ , and  $O_2$  over the experimental range of  $2 \times 10^{-4}$  to  $2 \times 10^{-3}$  torr. Within the experimental reproducibility the same value of  $\gamma$  was computed, with both  $N_2$  and  $O_2$ , when different metal surfaces were coated with the same vacuum grease even though the emissivities (table 2) and temperature increases at a given pressure (table 1) varied by a factor of three. Also, the Ar results are independent of the temperature of the transformer horn which varied markedly during the course of the experiments be-

Table 2  
Ratios of  $\gamma/\epsilon$  and translational thermal accommodation coefficients derived from the results in table 1 using eq. (5)<sup>a</sup>

Surface	$\gamma/\epsilon$		$\epsilon$		$\gamma$	
	$N_2$	$O_2$	Ar	$N_2$	$O_2$	Ar
Platinum uncoated	13.1	15.0	19.1	0.037	0.48	0.56
grease coated	4.2	4.2	4.6	(0.22)	(0.93)	(1.0)
carbon coated	0.91	0.94	0.92	1.0	0.91	0.94
Nickel uncoated	11.3	12.3	15.4	0.045	0.51	0.55
grease coated	10.0	10.1	10.8	(0.09)	(0.92)	(1.0)
Copper uncoated	21.3	27.9	29.1	0.02	0.43	0.56
grease coated	3.7	3.7	3.8	(0.26)	(0.97)	(1.0)

<sup>a</sup> Values in parenthesis were calculated from Ar results.



cause of the water cooling of the transducer. These findings support neglect of heat flow down the extension rod in eq. (2) – and, also, other assumptions implicit in the derivation of eq. (5) such as neglect of molecules striking the rod – because contributions from such additional energy transfer processes would vary with pressure or with  $\Delta T$  (which depends upon pressure).

Ratios of  $\gamma/\epsilon$  for  $N_2$  and  $O_2$  calculated from eq. (11) differ very little at small  $\Delta T$  from the values in table 2 which are obtained from eq. (5). However, when  $\Delta T \geq 0.18^\circ$  ratios of  $\gamma/\epsilon$  computed from eq. (11) are 6 to 108% higher than those in table 2. Ratios of  $\gamma/\epsilon$  computed from equation (11) for uncoated surfaces increase uniformly with gas pressure. The increases are of the order of 20%, ranging from 6% from  $N_2$  on nickel (where the pressure range covered is small) to 71% for  $O_2$  on copper. The fact that values of  $\gamma/\epsilon$  computed from eq. (5), but not from eq. (11), are invariant with pressure implies that rotational energy exchange is relatively small upon interaction of  $O_2$  and  $N_2$  with the uncoated surfaces and may be neglected in these room temperature measurements. Thus, the  $\gamma$  values in table 2 for uncoated surfaces correspond to  $\gamma$  (trans). The temperature rises of the greased surfaces are too small to distinguish between the applicability of eq. (5) and (11) except for  $N_2$  and  $O_2$  on grease-coated Ni where values of  $\gamma/\epsilon$  computed from eq. (11) increase by 23% and 14%, respectively, over the measured temperature range. This result suggests that rotational energy accommodation may be negligible on the greased surfaces also. The emissivity of the carbonized Pt surface is too high, and the measured temperature increase too small, to estimate the degree of rotational accommodation on this surface. One concludes that, in all cases, the thermal accommodation coefficients in table 2 may be interpreted as translational thermal accommodation coefficients.

The results in table 2 for argon on platinum are about 10% lower than those reported by Thomas and Brown [21] at 302 K using the low pressure method at  $2 \times 10^{-3}$  to  $3 \times 10^{-2}$  Torr. The difference probably is due to a difference in surface contamination, neither surface being "clean" by modern standards. Thomas [22] measurements of argon accommodation on clean tungsten surfaces at 303 K give values 2.5 to 3.0 times lower than the results of this work for argon on platinum, nickel, or copper. From the vacuum conditions employed one expects that the present measurements correspond to interaction of the test gas with adsorbed layer(s) of background gas and/or test gas. This conclusion is in accord with the observation that, for both  $N_2$  and  $O_2$ , the values of  $\gamma$  in table 2 are, within experimental error, the same on all three "uncoated" surfaces. It is interesting that Wachman [23] measured  $\gamma \approx 0.5$  for nitrogen on nitrogen covered tungsten, a value similar to those in table 2. Wachman [23] measured the thermal accommodation of  $N_2$  on tungsten in a tube without a getter and found that  $\gamma$  increased rapidly after flashing the surface in vacuum as a consequence of adsorption of contaminants and nitrogen on the tungsten filaments.

There is one other factor which might cause the vibration method to yield slightly different values of thermal accommodation coefficients than other methods. This arises because the velocity distribution seen by the oscillatory surface, averaged over

a cycle, is not Maxwellian. The velocity distribution leading to an apparent "temperature" of the incident molecules of  $E_i/2kT_i$  is not identical to the equilibrium velocity distribution characterized by that temperature. Since  $\gamma$  may depend upon the speed of the incident molecules [24] this difference in distribution could, in principle, lead to the measurement of a somewhat different thermal accommodation coefficient with a vibrating surface than with methods which sample a Maxwellian distribution. However, at the velocities achieved with the present apparatus, the apparent temperature of incident molecules is increased by such a small amount, a few degrees at most, that differences arising from the non-Maxwellian relative velocity distribution are immeasurable, as are changes in  $\gamma$  when the temperature of the test gas is raised over a few degrees.

#### Acknowledgements

We are indebted to Alan E. Crawford of Radyne, Ltd. for his assistance in the selection and design of the velocity transformer. This work was supported by the US Army Research Office, Durham.

#### References

- [1] H.Y. Wachman, J. Am. Rocket Soc. 32 (1966) 2.
- [2] M. Knudsen, Ann. Physik 34 (1911) 593.
- [3] L.B. Thomas and R.C. Golike, J. Chem. Phys. 22 (1954) 300.
- [4] Some previous evaluations of temperature jump heat conductivity data are based on assumptions of large mean free paths and Maxwell velocity distributions which did not exist under the experimental conditions. R.E. Harris, J. Chem. Phys. 46 (1967) 3217. discusses these assumptions and offers an alternative method of analyzing temperature jump results.
- [5] D.E. Klett and R.K. Irey, Advan. Cryogenic Engng. 14 (1968) 217.
- [6] F.M. Devienne, US Air Force Technical Report AF 61 (514), 818 (1956), AD 089497; J. Aeronautical Sci. 24 (1957) 403.
- [7] See articles in: Proc. Fifth Intern. Symp. on Rarefied Gas Dynamics, 1966, Vol. 1 (Academic Press, New York, 1967).
- [8] J.P. Harnett, in: Proc. Second Intern. Symp. on Rarefied Gas Dynamics, 1961 (Academic Press, New York, 1961) p. 1.
- [9] D.J. Mason, US Air Force Project RAND Report R-339 (1959).
- [10] S.A. Schaff, in: Univ. Michigan Heat Transfer Symposium (Univ. Michigan Press, Ann Arbor, Michigan, 1963) p. 261.
- [11] R.S. Lemons and G.M. Rosenblatt, Surface Sci. 48 (1975) 449.
- [12] H. Saltsburg, J.N. Smith and R.L. Palmer, in: The Structure and Chemistry of Solid Surfaces, Ed. G.A. Somorjai (Wiley, New York, 1969) p. 42–1.
- [13] G.M. Rosenblatt and R.S. Lemons, presented at Tenth Symp. New Mexico Chapter Am. Vacuum Soc., Santa Fe, N.M., 1974.
- [14] Details appear in the Doctoral Dissertation of R.S. Lemons, The Pennsylvania State University (1973), available from University Microfilms, Ann Arbor, Michigan.

- [15] E. Eisner, *J. Acoust. Soc. Amer.* 35 (1963) 1367.
- [16] A.E. Crawford, Radyne Ltd. Ultrasonics Group Technical Report No. 01-97, Wokingham, Berkshire, England, (Aug. 14, 1969).
- [17] R.W. Roberts and T.A. Vanderslice, *Ultrahigh Vacuum and Its Applications* (Prentice-Hall, Englewood Cliffs, N.J., 1963).
- [18] D.J. Santeler, D.H. Holkeboer, D.W. Jones and F. Pagano, *Vacuum Technology and Space Simulation* (NASA Publ. SP-105) (U.S. Govt. Printing Office, Washington, D.C., 1966).
- [19] R.L. Weber, *Temperature Measurement* (Edward Brothers, Ann Arbor, Michigan, 1941).
- [20] R.J. Thorn and G.H. Winslow, in: *Temperature, Its Measurement and Control in Science and Industry* (Reinhold, New York, 1962) Vol. III, part 1, p. 421.
- [21] L.B. Thomas and R.E. Brown, *J. Chem. Phys.* 18 (1950) 1367.
- [22] L.B. Thomas, in: *Proc. Fifth Intern. Symp. on Rarefied Gas Dynamics, 1966* (Academic Press, New York, 1967) p. 155.
- [23] H.Y. Wachman, in: *Proc. Fifth Intern. Symp. on Rarefied Gas Dynamics, 1966* (Academic Press, New York, 1967) p. 173.
- [24] F.O. Goodman and H.Y. Wachman, *J. Chem. Phys.* 46 (1967) 2376.